



ORIGINAL ARTICLE

Diagnostic Value of Multislice CT in differentiating Retroperitoneal Fat containing Masses in Adults

Amr Mohamed Teama¹, Ahmed Mohamed Elsayed², Emad Hasan Emara¹

¹Diagnostic and Interventional Radiology Department, Faculty of Medicine, Kafrelsheikh University, Kafrelsheikh, Egypt.

² Damanhur National medical institute, Radiology Department, Egypt.

*Corresponding author:

Amr Mohamed Teama

Email:

amr.teama@hotmail.com

Submit date:12-06-2025

Revise date:09-07-2025

Accept date:15-07-2025

ABSTRACT

Background: Retroperitoneal fat-containing masses present significant diagnostic challenges in clinical practice, encompassing benign entities and malignant neoplasms. This study evaluated the diagnostic accuracy of multislice computed tomography (CT) in differentiating adult retroperitoneal fat containing lesions through morphological characterization including lesions margins, borders, calcifications, enhancement criteria and tissue density analysis.

Methods: This retrospective observational study examined 78 patients aged 18-65 years of both sexes who underwent diagnostic CT examination of the abdomen and pelvis. Both non-contrast and contrast-enhanced multislice CT examinations were performed using a 16-slice scanner. Benign lesions were followed with serial imaging at six months, while suspicious malignant cases underwent histopathological correlation through surgical excisional biopsies.

Results: The cohort demonstrated a mean age of 56.35 ± 13.61 years. Adrenal adenomas represented the predominant pathology (49.9%), followed by renal angiomyolipomas (28%) and retroperitoneal liposarcomas (12.8%). Most cases presented as incidental findings (53.8%). Benign lesions exhibited mean maximum dimensions of 2.75 ± 1.95 cm with characteristic fat density averaging -42.25 ± 0.35 Hounsfield units. Six-month follow-up revealed stable disease in 77.5% of benign cases. Among ten liposarcomas, well-differentiated subtype predominated (50%), with CT demonstrating 90% diagnostic accuracy for liposarcoma identification with complete pathological confirmation.

Conclusions: Multislice CT demonstrates excellent diagnostic capability in characterizing retroperitoneal fat-containing masses, achieving high accuracy in distinguishing benign from malignant lesions through morphological assessment and density measurements.

Keywords: Adrenal Adenoma, Diagnostic Accuracy, Fat-Containing Masses, Liposarcoma, Retroperitoneal Masses.

INTRODUCTION

Retroperitoneal fat-containing masses in adults present a complex diagnostic challenge, encompassing a broad spectrum of pathologies from benign lesions such as lipomas and myelolipomas to malignant neoplasms including liposarcomas and lymphomas [1]. Accurate differentiation of these masses is crucial for appropriate clinical management and patient outcomes [2-4].

Despite the clinical importance of accurate diagnosis, certain diagnostic challenges persist [5, 6]. Well-differentiated versus dedifferentiated liposarcomas and benign versus malignant fat-containing tumors may exhibit overlapping imaging features, sometimes necessitating adjunctive imaging modalities and histopathological confirmation [7, 8]. Recent advances in radiomics and deep learning approaches have enhanced preoperative differentiation capabilities, improved diagnostic

confidence and supporting personalized management strategies [9].

The retroperitoneal space offers distinct imaging advantages due to the natural attenuation contrast between retroperitoneal fat and surrounding organs, which greatly improves diagnostic accuracy in detecting and characterizing pathology [10]. This natural contrast enables effective distinction between adipose tissue and skeletal muscle, bone, and parenchymal organs, while differentiating cortical from trabecular bone and visceral from subcutaneous fat distributions [11].

Multislice computed tomography (CT), particularly multidetector CT (MDCT), has emerged as the cornerstone imaging modality for evaluating retroperitoneal masses [2, 12]. The technology provides detailed assessment of lesion composition, including fat content, calcification patterns, necrotic components, and enhancement characteristics [11, 13]. This anatomical advantage positions CT as the preferred imaging modality for comprehensive retroperitoneal assessment [14, 15].

Based on these considerations, we hypothesized that MDCT represents an effective diagnostic tool for differentiating adult retroperitoneal fatty lesions. The objective of this study was to evaluate the diagnostic accuracy of MDCT in characterizing various adult retroperitoneal fatty lesions through comparative analysis of benign lesions with follow-up CT imaging and correlation of malignant cases with corresponding histopathological findings.

METHODS

Study design and setting:

This retrospective observational study involved 78 patients aged 18-65 years of both sexes who underwent diagnostic CT examination of the abdomen and pelvis at our hospital.

The study adhered to the ethical principles delineated in the Declaration of Helsinki (1964, last revised October 2013) [16].

Patients were excluded from the study if they had documented hypersensitivity reactions to contrast media, renal function impairment (serum creatinine levels exceeding 1.5 mg/dl) that contraindicated contrast administration without planned post-contrast dialysis, or if they were pregnant females at the time of examination.

Ethical considerations:

Institutional Review Board approval was obtained from the Research Ethics Committee of Kafrelsheikh University Faculty of Medicine prior to study initiation (ID: KFSIRB200-629). Informed consent was obtained from participants.

Clinical assessment and laboratory evaluation:

Comprehensive clinical histories were obtained for all participants, and previous imaging investigations were systematically reviewed. Renal function assessment was performed through standard laboratory tests to determine eligibility for contrast-enhanced imaging protocols.

Imaging protocol

MDCT examinations of the abdomen and pelvis were performed using a Siemens Go Now 16-slice CT scanner. Both non-contrast and intravenous contrast-enhanced studies were acquired according to standardized protocols.

Contrast administration protocol

The MDCT examination was conducted following a standardized protocol. An 18–20 gauge cannula was inserted into the right antecubital fossa for intravenous access, and a non-ionic contrast agent (Omnipaque 350) was administered using a power injector at a weight-adjusted dose of 1 ml/kg. The CT scan of the abdomen and pelvis, performed with intravenous contrast, employed the following parameters: 350 mA tube current, 120 kV tube voltage, 0.5-second rotation time, 5 mm slice thickness, 8 mm table feed, and 3 mm incremental image reconstruction. The scanning range extended from the diaphragm to the pubic symphysis, with patients positioned supine.

Following the scan, the peripheral venous line was removed, and the patient was observed for 15 minutes to monitor for any adverse reactions. Acquired images were transferred to a dedicated workstation for volumetric data analysis, including multiplanar reconstruction, and two- and three-dimensional reformations with volume rendering techniques, as clinically indicated.

Image analysis and interpretation:

Image analysis of retroperitoneal lesions was conducted based on anatomical and morphological characteristics, including lesion size, margin regularity (regular or irregular), border definition (smooth or sharp), and the presence or absence of calcifications, along with their distribution within the lesion. The enhancement pattern observed on imaging was assessed and categorized as homogeneous, heterogeneous, absent, or showing delayed enhancement. Lesion density was quantified by placing a circular region of interest (ROI) centrally within the lesion, encompassing the majority of its area. The CT scanner provided Hounsfield Unit (HU) values for each ROI, representing the average tissue density. These HU values were instrumental in tissue characterization, enabling differentiation among various types of retroperitoneal masses, such as cystic, solid, or fatty lesions, with the latter typically exhibiting lower HU values.

Histopathological correlation

Surgical excisional biopsies were obtained for 10 patients with imaging findings suspicious of malignancy. Histopathological analysis was conducted to provide definitive tissue diagnosis and correlation with radiological interpretations. The remaining 68 patients with benign imaging characteristics underwent six-month follow-up imaging surveillance.

Statistical analysis

SPSS version 20 software was utilized for data analysis. According to the type of data qualitative represent as number and percentage, quantitative continues group represent by mean \pm SD, the following tests were used to test differences for significance, difference and association of qualitative variable by Chi square test. Differences between quantitative independent groups by t test or Mann Whitney test. The P value was set at ≤ 0.05 for significant results.

RESULTS

The cohort comprised 78 patients with mean age 56.35 ± 13.61 years. Adrenal adenomas represented the predominant pathology (49.9%) with left adrenal adenoma was majority with 28.2% followed by right adrenal adenoma with 21.7%, followed by retroperitoneal liposarcomas (12.8%) and renal angiomyolipomas (28%). Most cases presented as incidental findings (53.8%). Table 1

Benign lesions demonstrated mean maximum dimensions of 2.75 ± 1.95 cm with characteristic fat density averaging -42.25 ± 0.35 Hounsfield units. Six-month follow-up revealed stable disease in 77.5% of cases, with size increase observed in 20.1%. Table 2

Among ten liposarcomas, well-differentiated subtype predominated (50%), with dedifferentiated variants comprising 40%. Metastatic disease occurred in 50% of cases. CT demonstrated 90% diagnostic accuracy for liposarcoma identification with complete pathological confirmation. Table 3

Benign lesions showed comparable stability rates between adrenal (79.1%) and renal (76.0%) locations at follow-up. Size progression occurred more frequently in renal lesions (24%) compared to adrenal lesions (16.3%), though differences were statistically insignificant ($P=0.18$). Table 4

Table 1: Patient demographics and clinical presentation

	n=78	
Age (years)	56.35±13.61 range (20-81)	
Primary findings distribution	Left adrenal adenoma	22 (28.2%)
	Right adrenal adenoma	17 (21.7%)
	Retroperitoneal liposarcoma	10 (12.8%)
	Left renal angiomyolipoma	8 (10.2%)
	Right renal angiomyolipoma	8 (10.2%)
	Renal exophytic angiomyolipoma	6 (7.6%)
	Left adrenal myelolipoma	4 (5.1%)
	Bilateral renal angiomyolipomas	3 (3.8%)
Clinical presentation	Incidental finding	42 (53.8%)
	Abdominal swelling	12 (15.3%)
	Left renal dull aching pain	8 (10.2%)
	Bilateral flank swelling	6 (7.6%)
	Left loin pain	6 (7.6%)
	Sudden weight loss	4 (5.1%)

Data was presented as mean ± SD or frequency (%).

Table 2: Radiological characteristics and measurements

Maximum dimension of benign lesions (cm) (n=68)		2.75 ± 1.95
Hounsfield Units (HU) (n=78)		-42.25 ± 0.35
Follow-up at 6 months	No change	53 (77.5%)
	Increased size	13 (20.1%)
	Decreased size	2 (2.4%)

Data was presented as mean ± SD or frequency (%).

Table 3: Malignant lesion characteristics and pathological correlation

Liposarcoma Subtypes (n=10)	Well-differentiated liposarcoma	5 (50%)
	De-differentiated liposarcoma	4 (40%)
	Malignant fatty retroperitoneal lesion	1 (10%)
Metastasis Status	Present	5 (50%)
	Absent	5 (50%)
CT Diagnostic Accuracy	CT diagnosed as liposarcoma	9 (90%)
	CT diagnosed as fatty lesion	1 (10%)
Pathologically confirmed liposarcoma		10 (100%)

Data was presented as frequency (%).

Table 4: Follow-up outcomes by anatomical location

Benign lesions (n=68)	Adrenal lesions	Renal lesions	Total	P value
Same size	34 (79.1%)	19 (76.0%)	53 (77.5%)	P = 0.18
Decreased size	2 (4.6%)	0 (0%)	2 (2.3%)	
Increased size	7 (16.3%)	6 (24%)	13 (20.1%)	
Total	43 (100%)	25 (100%)	68 (100%)	

Data was presented as frequency (%).

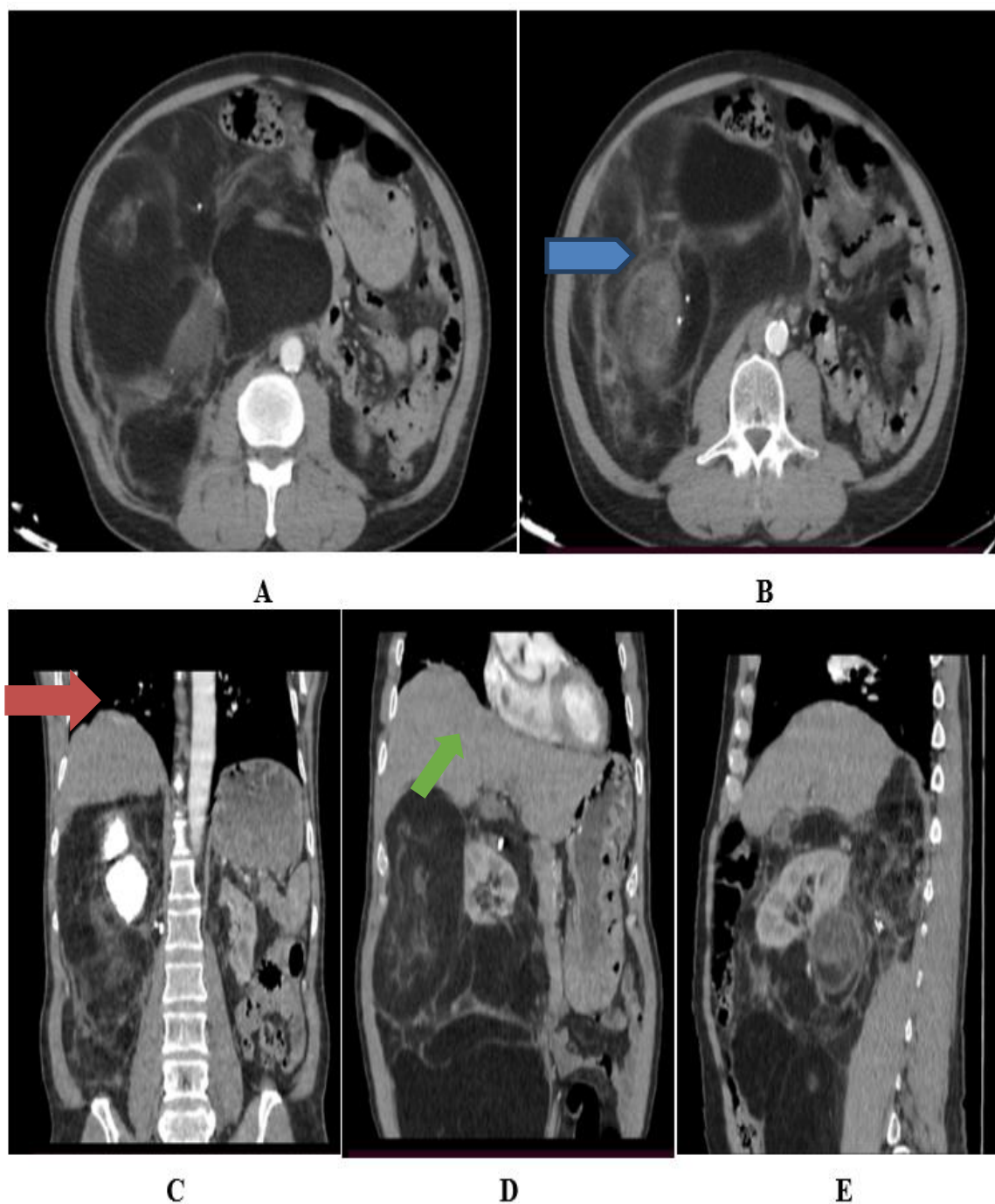


Figure 1: (A-E)

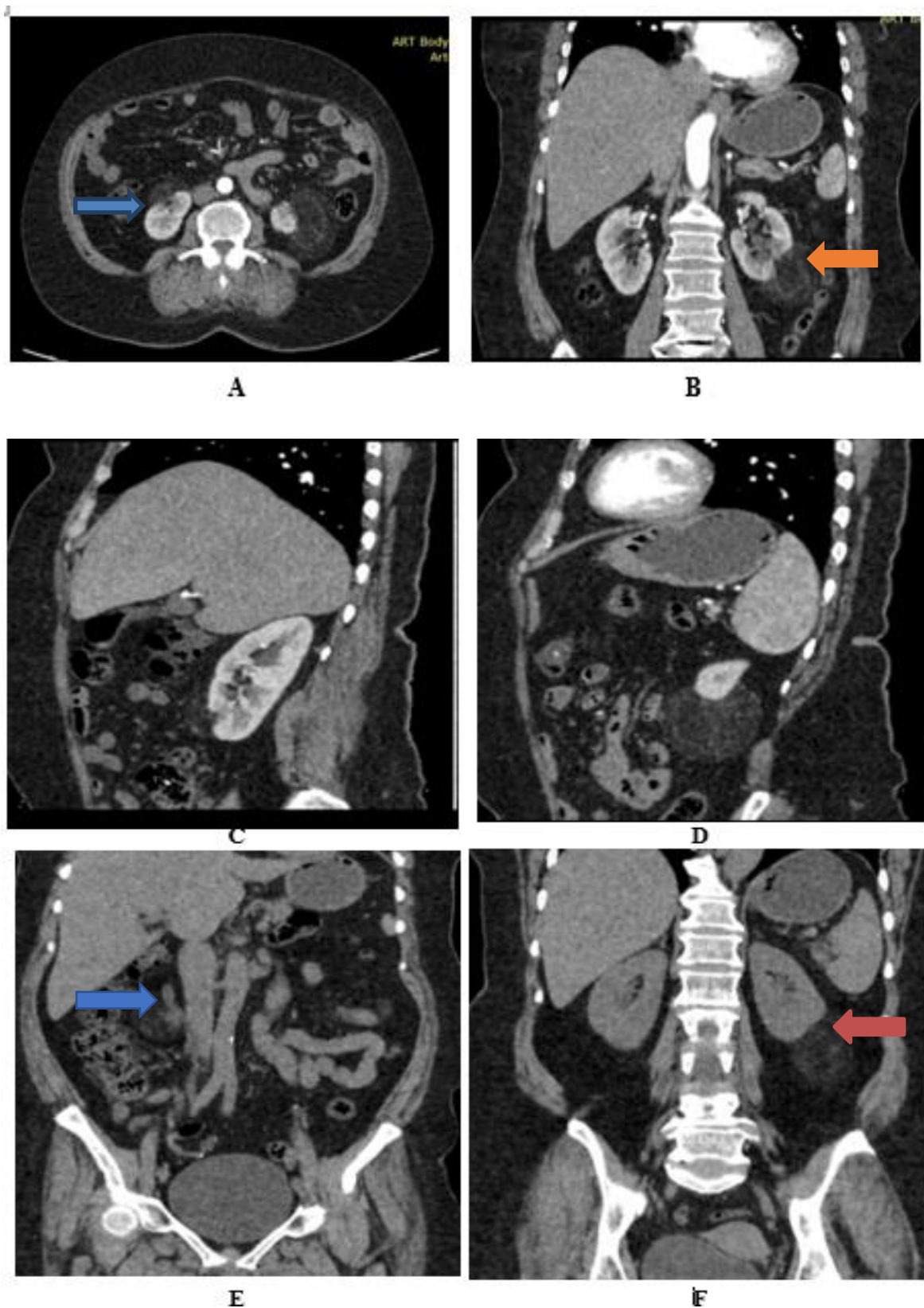


Figure 2: (A-F)

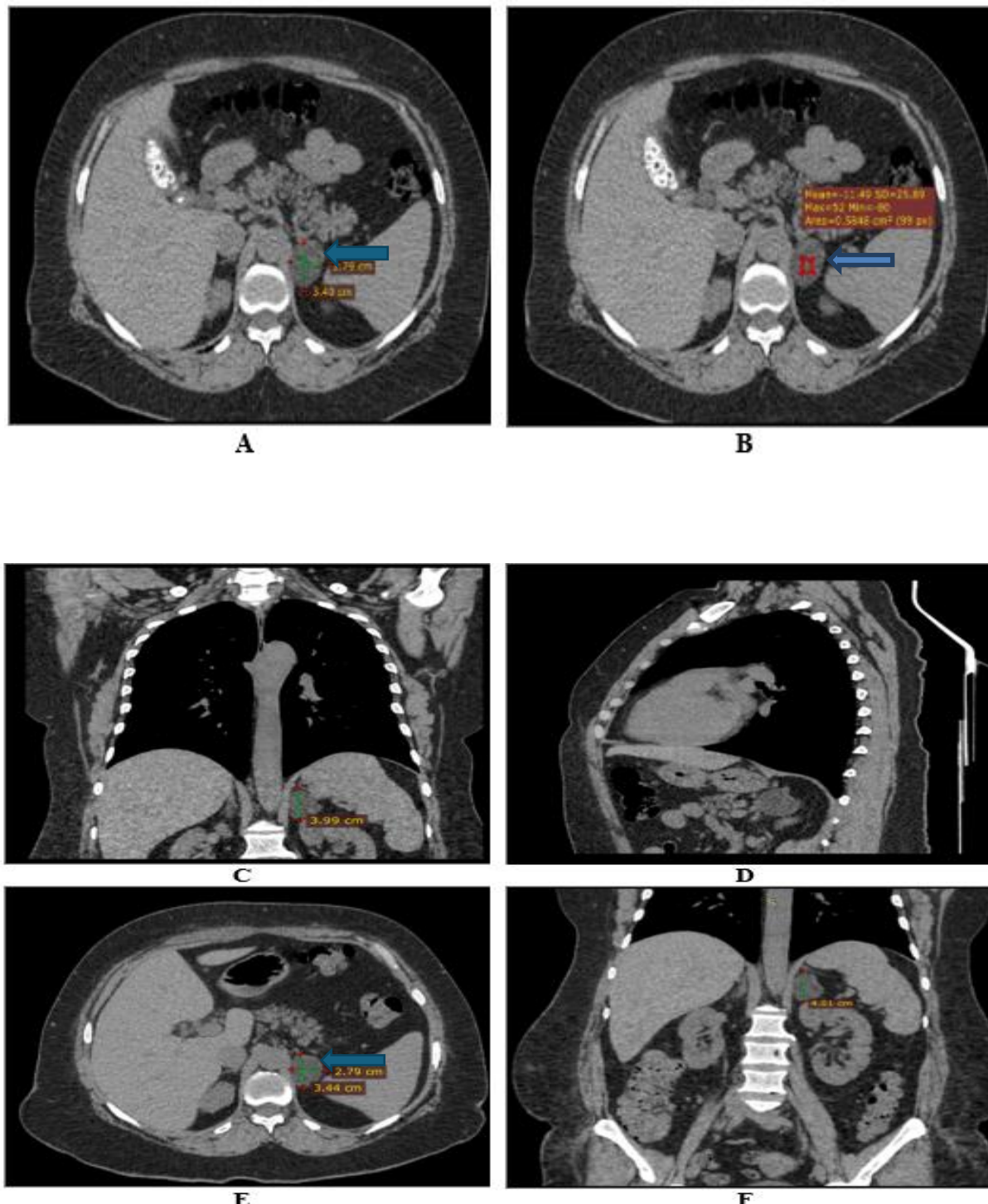


Figure 3: (A-F)

DISCUSSION

The present study demonstrates a characteristic profile for retroperitoneal fat-containing masses, with a mean patient age of 56.35 ± 13.61 years and a predominance of incidental findings (53.8%). This demographic pattern aligns closely with previous investigations,

though notable variations exist in age distribution. Anwar and AbdelKadir [17] reported a considerably younger cohort with a mean age of 41.5 ± 22.8 years, ranging from 4 months to 81 years, which may reflect their broader inclusion criteria encompassing both fat-containing and non-fat-containing retroperitoneal masses.

The younger age range in their study likely results from the inclusion of pediatric cases and a more diverse pathological spectrum, whereas our focused evaluation of fat-containing lesions naturally selects for an older population where adrenal adenomas and angiomyolipomas are more prevalent.

The predominance of adrenal adenomas in our cohort (49.9%, with left-sided predominance at 28.2% versus right-sided at 21.7%) represents a significant finding that reflects the natural history of these lesions in the adult population. This distribution pattern differs markedly from Anwar and AbdelKadir [17] findings, where lymphomas and liposarcomas each represented 19.2% of malignant cases, while adrenal myelolipomas comprised only 22.2% of benign lesions. The high incidence of incidental detection (53.8%) in our series underscores the increasing frequency of cross-sectional imaging and the need for accurate characterization of these lesions to avoid unnecessary interventions.

The radiological characteristics observed in our study provide valuable quantitative parameters for diagnostic differentiation. Benign lesions demonstrated mean maximum dimensions of 2.75 ± 1.95 cm with characteristic fat density averaging -42.25 ± 0.35 Hounsfield units. These measurements align well with established diagnostic criteria outlined by Shaaban et al. [18], who emphasized that fat-containing retroperitoneal lesions are primarily identified by their characteristic fat attenuation ranging from -10 to -100 HU. Our measured fat density values fall well within this established range, supporting the reliability of CT densitometry in lesion characterization.

The stability observed in 77.5% of cases during six-month follow-up, with size increase noted in 20.1%, provides important prognostic information for clinical management. This stability pattern is consistent with the benign nature of most fat-containing retroperitoneal masses

and supports conservative management approaches for appropriately characterized lesions. The size progression observed in a minority of cases emphasizes the importance of surveillance imaging, particularly given that size increase may indicate malignant transformation or growth of initially undetected malignant components.

Our analysis of ten liposarcomas revealed a predominance of well-differentiated subtypes (50%) with dedifferentiated variants comprising 40%, which closely mirrors the distribution patterns reported in the literature. The 90% diagnostic accuracy achieved for liposarcoma identification with complete pathological confirmation represents a significant advancement over previous studies. Feng et al. [19] reported an overall diagnostic accuracy of 98.33% for all retroperitoneal masses using multi-slice spiral CT, though their study included a broader spectrum of lesions. The high accuracy in our focused evaluation of fat-containing masses suggests that CT characteristics are particularly reliable for liposarcoma diagnosis when appropriate imaging protocols are employed.

The occurrence of metastatic disease in 50% of liposarcoma cases in our series highlights the aggressive potential of these neoplasms and the critical importance of accurate initial staging. This metastatic rate is consistent with the natural history of retroperitoneal liposarcomas, which have a propensity for local recurrence and distant metastasis. Zheng et al. [20] identified specific CT features associated with malignancy, including ill-defined margins, irregular surfaces, and larger dimensions, which complement our findings regarding the diagnostic reliability of CT in characterizing these lesions.

The comparative analysis of stability rates between adrenal (79.1%) and renal (76.0%) lesions provides valuable insights into the natural history of fat-containing masses at different

anatomical sites. The slightly higher progression rate observed in renal lesions (24%) compared to adrenal lesions (16.3%), may reflect the different pathophysiological processes underlying angiomyolipomas versus adrenal adenomas. This finding is particularly relevant given that renal angiomyolipomas have a recognized potential for growth and complications, including spontaneous hemorrhage in larger lesions.

Comparable stability rates between anatomical locations support the reliability of CT-based surveillance strategies regardless of lesion location. However, the trend toward higher progression rates in renal lesions suggests that location-specific follow-up protocols may be warranted. Shaaban et al. [18] noted that renal angiomyolipomas are mostly fatty but that minimal-fat variants appear hyperattenuating and may resemble papillary renal cell carcinoma, emphasizing the importance of careful characterization and appropriate follow-up for renal fat-containing lesions.

The overall diagnostic performance demonstrated in our study compares favorably with previous investigations while providing specific insights into fat-containing retroperitoneal masses. Shalaan et al. [21] reported moderate diagnostic accuracy with exact or two-differential match achieved in 69.7% of cases for all retroperitoneal lesions, while our focused approach to fat-containing masses achieved superior diagnostic reliability. This enhanced performance likely reflects the more specific imaging characteristics of fat-containing lesions and the refined diagnostic criteria applied in their evaluation.

This retrospective study presents several limitations that may affect generalizability. The single-center design from one institution restricts broader applicability. The relatively small sample size, particularly the limited number of malignant cases, may reduce statistical power for comprehensive subgroup

analyses. The six-month follow-up period may be insufficient to detect long-term changes in lesion behavior. Additionally, selection bias may exist as only patients undergoing CT examination were included, potentially excluding cases managed through alternative imaging modalities or conservative approaches.

Conclusions:

Multislice CT appears to offer excellent diagnostic capability in characterizing retroperitoneal fat-containing masses, achieving high accuracy in distinguishing benign from malignant lesions through morphological assessment and density measurements in this retrospective single-center study. Further prospective multicenter studies would be beneficial to validate these findings across diverse patient populations.

Figure legends:

Case 1:

Female patient 55 years old complaining from rapidly growing right side of the abdomen.

Contrast enhanced CT axial (A&B), coronal reformatted images (C&D), & sagittal reformatted image (E) of the abdomen and pelvis showing: Huge right abdominal retroperitoneal encapsulated fat density lesion (-90 HU) measuring approximately 23 x 20 x 19 cm at maximum cranio-caudal, transverse & AP diameters respectively. The fore mentioned lesion is seen extending from the level of the sub-hepatic region down to the right pelvic region. The lesion is seen encircling but not invading the right kidney (green arrow) which is displaced anteriorly and malrotated with its hilum facing posteriorly. Dense coarse large calcific regions (orange arrow) and multiple intervening enhancing septa are seen within the lesion with one of them mounting to mass formation (blue arrow) measuring 7.4 x 6.3 cm. No enlarged abdominal, retroperitoneal or pelvic nodes are noted. The lesion is histopathological proven to be differentiated liposarcoma.

Case 2:

Female patient came for further CT assessment after sonographic finding of left renal mass.

On her first assessment CT with contrast was done (axial A, Coronal B and sagittal C & D) revealed bilateral well defined exophytic fat density renal lesions from both kidneys lower poles, the one on the right kidney (blue arrow) was measuring 4.7 x 2.3 x 4.4 at maximum CC, AP & transverse diameters & on the left kidney (orange arrow) was measuring 6 x 6.7 x 4 at maximum CC, AP & transverse diameters respectively. Both lesions showed fatty attenuation with -91 HU for the right one and -83 HU for the left one and characteristic claw sign confirming renal origin. Both showed no internal calcifications. NO detected abdominal or retroperitoneal enlarged lymph nodes. The following characteristics kept with bilateral exophytic renal angiomyolipomas.

Follow up non contrast CT study was done 6 months later: (coronal non contrast CT abdomen and pelvis E & F) showed rather stationary coarse for both lesions now measuring 4.5 x 2.5 x 4.2 cm for the right (blue arrow) & 6.2 x 6.5 x 3.8 cm for the left one (orange arrow) at maximum CC, AP & transverse diameters respectively.

Case 3:

A 46-year-old female patient underwent chest computed tomography for evaluation of fever and chest tightness. Non-contrast enhanced MDCT (axial images (Figures A-B), coronal (Figure C), and sagittal (Figure D) reformatted images) incidentally identified a left adrenal gland nodule measuring 2.8 × 3.4 × 4.0 cm in maximum dimensions. The lesion exhibited hypodense attenuation characteristics with mean Hounsfield unit values of -11 on non-contrast images, consistent with fatty content (blue arrow). The imaging features were most compatible with incidental left adrenal adenoma. **Six-month follow-up non-contrast CT** examination of the abdomen and pelvis demonstrated stable lesion size

(blue arrow) without significant interval change (Figures E-F), supporting the benign nature of the adrenal adenoma.

Financial support and sponsorship: Nil

Conflict of Interest: Nil

REFERENCES

1. Drylewicz MR, Lubner MG, Pickhardt PJ, Menias CO, Mellnick VM. Fatty masses of the abdomen and pelvis and their complications. *Abdom Radiol*. 2019;44:1535-53.
2. Chinwan D, Vohra P. Role of multi detector computed tomography in the evaluation of retroperitoneal masses. *Int J Res Med Sci*. 2018;6:3949-53.
3. Nayak PK, Rao M, Jena SK, Kumar BA. A clinical study to evaluate the role of CT in the detection, localization and characterization of retroperitoneal masses. *Panacea J Med Sci*. 2023;13:222-6.
4. Sangster GP, Migliaro M, Heldmann MG, Bhargava P, Hamidian A, Thomas-Ogunniyi J. The gamut of primary retroperitoneal masses: multimodality evaluation with pathologic correlation. *Abdom Radiol*. 2016;41:1411-30.
5. Morosi C, Stacchiotti S, Marchianò A, Bianchi A, Radaelli S, Sanfilippo R, et al. Correlation between radiological assessment and histopathological diagnosis in retroperitoneal tumors: Analysis of 291 consecutive patients at a tertiary reference sarcoma center. *Eur J Surg Oncol*. 2014;40:1662-70.
6. Zhang J, Yu X, Song Y, Zhang H, Chen Y, Ouyang H, et al. Comparison of imaging and pathologic findings of retroperitoneal dedifferentiated liposarcoma. *Chin J Oncol*. 2019;41:223-8.
7. Xu J, Miao L, Wang C-x, Wang H-h, Wang Q-z, Li M, et al. Preoperative contrast-enhanced CT-based deep learning radiomics model for distinguishing retroperitoneal lipomas and well-differentiated liposarcomas. *Acad Radiol*. 2024;31:5042-53.
8. Lahat G, Madewell JE, Anaya DA, Qiao W, Tuvlin D, Benjamin RS, et al. Computed tomography scan-driven selection of treatment for retroperitoneal liposarcoma histologic subtypes. *Cancer*. 2009;115:1081-90.
9. Xu J, Guo J, Yang H-q, Ji Q-l, Song R-j, Hou F, et al. Preoperative contrast-enhanced CT-based radiomics nomogram for differentiating benign and malignant primary retroperitoneal tumors. *Eur Radiol*. 2023;33:6781-93.

10. Chu JS, Wang ZJ. Protocol optimization for renal mass detection and characterization. *Radiol Clin*. 2020;58:851-73.
11. Mazonakis M, Damilakis J. Computed tomography: What and how does it measure? *Eur J Radiol*. 2016;85:1499-504.
12. Rajiah P, Sinha R, Cuevas C, Dubinsky TJ, Bush Jr WH, Kolokythas O. Imaging of uncommon retroperitoneal masses. *Radiographics*. 2011;31:949-76.
13. Caraianni C, Yi D, Petrescu B, Dietrich C. Indications for abdominal imaging: When and what to choose? *J Ultrason*. 2020;20:e43-e54.
14. Messiou C, Moskovic E, Vanel D, Morosi C, Benchimol R, Strauss D, et al. Primary retroperitoneal soft tissue sarcoma: Imaging appearances, pitfalls and diagnostic algorithm. *Eur J Surg Oncol*. 2017;43:1191-8.
15. Porrello G, Cannella R, Randazzo A, Badalamenti G, Brancatelli G, Vernuccio F. CT and MR imaging of retroperitoneal sarcomas: A practical guide for the radiologist. *Cancers*. 2023;15:2985.
16. Helsinki F. Declaration of Helsinki World Medical Association Declaration of Helsinki. *Bull World Health Organ*. 2013;79:373-4.
17. Anwar DSE, AbdelKadir RMA. The role of multidetector computed tomography in characterization and differentiation of retroperitoneal masses. *Zagazig Univ Med J*. 2023;29:525-31.
18. Shaaban AM, Rezvani M, Tubay M, Elsayes KM, Woodward PJ, Menias CO. Fat-containing retroperitoneal lesions: Imaging characteristics, localization, and differential diagnosis. *Radiographics*. 2016;36:710-34.
19. Feng Y, Zhang W, Luo C. Analysis of the clinical value of multi-slice spiral computed tomography (MSCT), magnetic resonance imaging (MRI) and ultrasound (US) in the diagnosis of retroperitoneal tumors. *Transl Cancer Res*. 2021;10:2247-54.
20. Zheng Z, Zhao X, Zhao Y, Yang L, Zhao J, Dai J, et al. Evaluation of CT findings for the differentiation of benign from malignant primary retroperitoneal tumors. *Chin Med J*. 2014;127:114-9.
21. Shalaan A, Refaat M, Farouk H, Saleh GS. Role of multislice computed tomography in characterization of different retroperitoneal masses. *TantaMedJ*. 2017;45:1-7.

Citation

Teama, A., Elsayed, A., Emara, E. Diagnostic Value of Multislice CT in differentiating Retroperitoneal Fat containing Masses in Adults. *Zagazig University Medical Journal*, 2025; (4786-4796): -. doi: 10.21608/zumj.2025.392341.3992